■ Materials Science inc. Nanomaterials & Polymers

Development of an Ionic Liquid Based Method for the Preparation of Albumin Nanoparticles

Begüm Demirkurt and Yasar Akdogan*[a]

Albumin based nanocarriers have been widely used in drug delivery studies. Here, we developed a water-in-ionic liquid (IL) emulsion-like method to prepare bovine serum albumin (BSA) nanoparticles as alternative to the traditional organic solvents containing techniques. Conformational changes of albumin induced by the imidazolium based ILs at the water-IL interface triggers the BSA nanoparticle formation. The albumin nanoparticle formation are dependent on the experimental parameters and the hydophobicity of the IL. At pH 9.0, using 1.3%wt of BSA in water/1-butyl-3-methyl imidazolium tetrafluoroborate (BmimBF$_4$) (50/50 mol%) and TX-100/butanol surfactant mixture yields uniformly distributed 200 nm average sized BSA nanoparticles. Different than BmimBF$_4$, using a more hydrophilic IL, EmimBF$_4$ yielded albumin aggregates. Instead, using a more hydrophobic IL, HmimBF$_4$ produced albumin nanoparticles but a non-uniform size distribution was obtained. These results indicate that the ionic liquids called green and designer solvents can be also used to synthesize albumin nanoparticles.

Introduction

Nanoparticles have been used as drug carriers for a long time. Among all possible different nanocarriers, albumin based nanoparticles have been extensively studied due to their unique properties such as biodegradability, lack of toxicity and antigenicity, and easy preparation.[1] Also, high drug binding capacity of albumin for both hydrophilic and hydrophobic drugs has inspired scientists to prepare drug nanocarriers from albumin protein.[2,3] In addition, the albumin nanoparticle is an attractive candidate for the site-specific delivery of drugs in the body. The possibility of ligand binding on the surface of albumin nanoparticles leads to a specific accumulation in the targeted cells, e.g. tumor cells.[4,5] Also, binding of albumin to albumin binding proteins, 60kDa glycoprotein (gp60) and secreted protein, acidic and rich in cysteine, (SPARC) enhances uptake of albumin nanoparticles by tumors.[6,7]

Formation of albumin nanoparticles is triggered by both decreasing protein intramolecular interactions and increasing protein unfolding. Changing the conditions of medium such as ionic strength, pH, temperature and type of solvent leads to albumin conformational changes, and thus they may result in nanoparticle formation. There are two main methods to prepare albumin nanoparticles; desolvation and emulsification methods. In the desolvation process, addition of organic solvents such as ethanol, methanol or acetone reduces the solubility of the protein in water and leads to nanoparticle formation under constant stirring.[8,9] In the presence of cross-linker such as glutaraldehyde, stable albumin nanoparticles were obtained in the size range of 150–280 nm.[8] Yet, the used volatile, flammable and toxic organic solvents are harmful for the environment. Also, the waste of them causes storage problems.

In the emulsification method, the aqueous solution of albumin is emulsified in oil phase (castor oil, cyclohexane, dichloromethane, etc.) by using a high-speed homogenizer, high-pressure homogenizer or ultrasonic shear.[10–12] Thermal heating or a cross-linker can be used for the stabilization of the albumin nanoparticles with the help of surfactants.[10,11] For example, BSA nanoparticles (600 nm) were synthesized by using emulsion-heat stabilization technique. The mixture of basic BSA aqueous solution and castor oil/SPAN-80 was emulsified by a high-speed homogenizer.[10] In the other study, BSA aqueous solution was added into cyclohexane/SPAN-80 mixture and then homogenizer was applied to obtain BSA nanoparticles (400 nm).[11] Also, human serum albumin (HSA) nanoparticles (130 nm) obtained by emulsification-solvent evaporation process have been used clinically for the delivery of paclitaxel, Abraxane® approved by the U.S. Food and Drug Administration (FDA) in 2005, against breast cancer.[13]

Although, traditional organic solvents have been commonly used in desolvation and emulsification methods, alternatively, in this study we used ionic liquids (ILs) to synthesize bovine serum albumin (BSA) nanoparticle. Ionic liquids are melted salts with melting points below 100 °C, often below room temperature. Their unique properties have made them alternative solvents to traditional organic solvents in different fields such as organic synthesis, catalysis, electrochemistry, purification, pharmacology, etc.[14,15] Since they are non-volatile, non-flammable and recyclable, they are called green solvents.[16] Therefore, synthesizing albumin nanoparticles in an IL based system instead of using organic solvents provides a more environmental friendly synthesizing technique. In addition, physical properties of ILs such as polarity, miscibility, density and

[a] B. Demirkurt, Dr. Y. Akdogan
     Materials Science and Engineering Department
     İzmir Institute of Technology
     35430 Urla, İzmir, Turkey
     E-mail: yasarakdogan@iyte.edu.tr

viscosity can be tuned by selection different anions and cations. Therefore, ILs are also referred to as designer solvents.[17]

Serum albumin is a transporter protein for soluble and insoluble compounds in blood. Several drugs binds to BSA at two primary binding sites (site I and site II).[18–21] Its globular structure with three main domains consists of at least 67% alpha helical structure (Figure 1 (A)).[22] The segments of serum
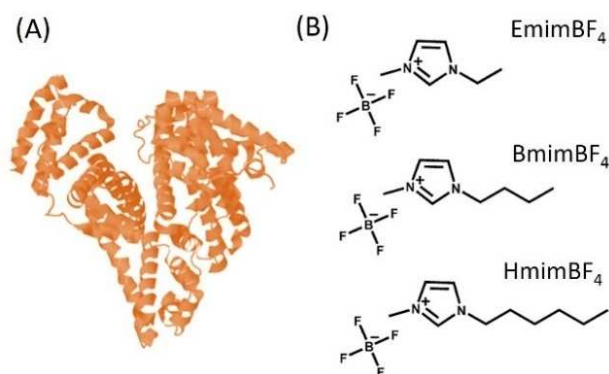
**Figure 1.** (A) Crystal structure of bovine serum albumin (BSA) (pdb-ID: 3v03).[22] (B) Chemical structures of imidazolium based ionic liquids (ILs): EmimBF$_4$, BmimBF$_4$ and HmimBF$_4$.

albumin are connected to each other through hydrogen bonds and electrostatic or hydrophobic interactions. They may lose their connections if the interaction to the ILs is favored. Interactions between ILs and albumin are affected by the kinds of anions and cations in ILs. For example, imidazolium based ionic liquids have denaturation effects on the albumin, but choline based ionic liquid such as choline dihydrogen phosphate (dhp) has a stabilizing effect on the albumin structure.[23,24] The denaturing effect of the ILs could be used to initiate albumin nanoparticle formation. Therefore, the chosen anions and cations regulate the albumin nanoparticle formation and affect the physical properties of albumin nanoparticles such as size, size distribution, morphology and stability. Also, for drug transportation, especially for the poor water-soluble drugs, ILs could be very effective to obtain drug loaded albumin nanoparticles in the future. Different types of drugs are soluble in ILs depending on the anions and cations.[17] This could help in encapsulating drugs in the albumin nanoparticle during the nanoparticle preparation. For these reasons, we aim to prepare albumin nanoparticles in an IL based system.

In the literature, ionic liquids have been used in emulsion/microemulsion systems for the replacements of aqueous phase, oil phase or surfactant molecules.[25] For example, starch nanoparticles were prepared separately in IL/oil, water/IL and water/oil (IL is surfactant) microemulsion systems.[26–28] Differently, in this work, we developed an emulsion-like technique by using imidazolium based ionic liquids to obtain albumin nanoparticles. We chose three 1-alkyl-3-methylimidazolium tetrafluoroborate, C$_n$mimBF$_4$, ionic liquids with different alkyl chain lengths, n = 2, 4, and 6: 1-ethyl-3-methylimidazolium tetrafluoroborate (EmimBF$_4$), 1-butyl-3-methylimidazolium tetrafluorobo-

rate (BmimBF$_4$) and 1-hexyl-3-methylimidazolium tetrafluoroborate (HmimBF$_4$), respectively (Figure 1 (B)). Increasing the length of alkyl chain of imidazolium cation increases the hydrophobicity of the IL.[29,30] This leads to a polar/nonpolar nanophase separation in the structure of IL. Therefore, addition of water into ILs that have biphasic structures results in the water aggregation.[30–34] Here, we showed that mixtures of ILs and albumin aqueous solution in the presence of surfactants and glutaraldehyde yield albumin nanoparticles after applying a high-speed homogenizer in the formed water pools (Figure 2). Parameters such as pH, BSA concentration, water
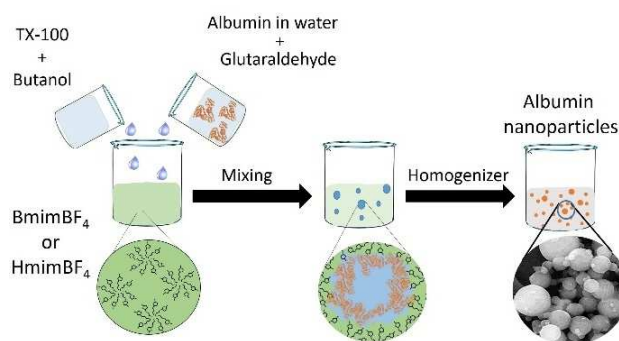
Figure 2. Schematic representation of BSA nanoparticle synthesis using water-in-IL emulsion-like technique.

volume, glutaraldehyde, surfactant and co-surfactant, and the effect of alkyl side chain lengths which strongly influence the BSA nanoparticle formation were studied in detail.

Results and Discussion

In C$_n$mimBF$_4$ ionic liquids with n > 4, aggregation of the hydrophobic alkyl side chains of imidazolium ring leads to a nanophase separation from ionic domains consisting of the imidazolium ring and the anion.[30] Therefore, a micelle-like structure is observed. For the water-IL binary system, polar water molecules can interact with ionic domains of C$_n$mimBF$_4$. For example, by addition of water into the BmimBF$_4$, water molecules are first dissolved and then form water aggregates around the ionic domains of BmimBF$_4$ especially for the intermediate water contents (50 mol%).[32–34] Although, these water rich domains can be investigated by ^{1}H NMR spectroscopy,[34] their sizes could not be detected by DLS in here due to their dynamic and swinging structures. Since the mixture of C$_n$mimBF$_4$, n > 4, and water form unstable mesostructures composed of water-rich and IL-rich domains, we developed an emulsion-like method to synthesize albumin nanoparticles in the water-in-ionic liquid (w/IL) system. For albumin nanoparticle preparation, various experimental parameters and the effect of alkyl side chains of ILs were studied in detail.

Effect of pH value on the albumin nanoparticle formation

The influence of aqueous phase pH value on the nanoparticle formation was studied with three different pH values including pH 4.0, 7.0 and 9.0. First, 12 mg of BSA aqueous solution (with glutaraldehyde) in 285 μL water was prepared at pH 4.0 and then mixed with $BmimBF_4$ solution in the presence of surfactant (TX-100) and co-surfactant (1-butanol). After that, high speed homogenizer was applied to obtain BSA nano-particles. But, at pH 4.0, BSA aggregation was observed. SEM image of this aggregation was shown in Figure S1 (A). Next, BSA aqueous solution was prepared at pH 7.0 and then mixed with $BmimBF_4$. After following the same procedure, a limited number of BSA nanoparticles in a film-like BSA structure was detected in the SEM images (Figure S1 (B) and (C)).

On the other hand, further increasing the pH value of BSA solution to 9.0, and then mixing with $BmimBF_4$ yielded BSA nanoparticles with regular spherical shapes (Figure 3 (A) and
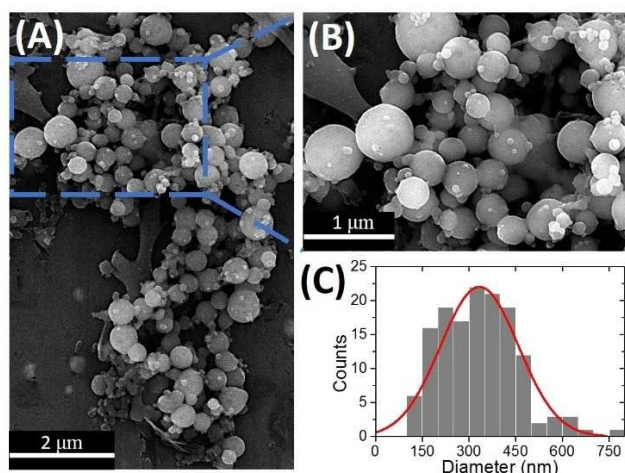
Figure 3. (A, B) SEM images of BSA nanoparticles prepared by addition of 12 mg BSA aqueous solution (285 μL) at pH 9.0 to the $BmimBF_4$ (3 g) based system. (C) Particle size distribution obtained from the SEM image (A). Final BSA concentration is 0.06 mM. Mol% of water and $BmimBF_4$ are 53% and 44%, respectively.
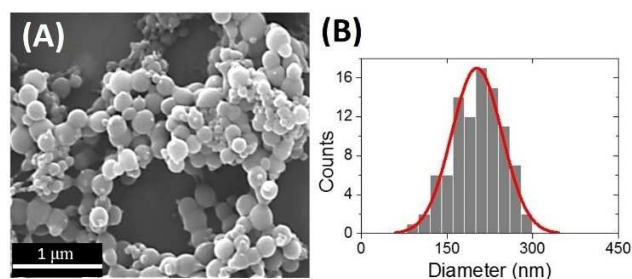
(B)). Figure 3 (C) shows the particle size distribution obtained from the SEM image in Figure 3 (A). The average size of albumin nanoparticles is 330 nm with a size distribution between 150 and 600 nm. In addition, DLS provides their average size as around 520 nm in solution with a PDI 0.271 (Figure S2 (A)). Also, the zeta potential of the BSA nanoparticles was found as −11 mV. Obtaining higher average particle size in solution by DLS is reasonable due to the formation of hydration shell and/or swelling nanoparticles with water.

These observations are in good agreement with the earlier works in which smaller albumin nanoparticles were obtained at pH 8.0 - 9.0 with the desolvation technique.[8,35] The influence of pH on the isolated albumin nanoparticle formation can be explained by the charge effects. Although, the structure of albumin remains stable between pH values of 4.0 and 9.0, the

charge of albumin changes from positive to negative with reported isoelectric points in the range from 4.8 to 5.6.[36] At pHs 4.0, 7.0 and 9.0, the reported charges of BSA are +10, −13, and −26, respectively.[36] The absolute value of charge of BSA at pH 9.0 is about twice the absolute value of charges of BSA at pH 4.0 and 7.0. Therefore, higher electrostatic repulsive forces at pH 9.0 keep the formed albumin nanoparticles away from each other which avoids the agglomeration. In addition, the albumin nanoparticle formation can be affected by the types of intermolecular interactions between $BmimBF_4$ and BSA which are also pH dependent. In addition to hydrogen bonding and hydrophobic interactions which exist between $[Bmim]^+$ and BSA, a higher electrostatic attraction between $[Bmim]^+$ and BSA takes place at pH 9.0 due to a net higher negative charge on albumin. At pH 9.0, the combination of these forces possibly supports the albumin nanoparticle formation and stabilization.

Effect of BSA concentration on the albumin nanoparticle formation

Effect of BSA concentration (in 285 μL water, at pH 9.0) on the size of BSA nanoparticles was studied with 0.5, 4 and 12 mg of BSA. Addition of 12 mg BSA (0.6 mM, 4 wt% in water) containing water into $BmimBF_4$ yielded BSA nanoparticles (average 330 nm) with a size distribution between 150 and 600 nm (Figure 3). In order to obtain smaller nanoparticles with a narrower size distribution, we decreased the BSA content from 12 mg to 4 mg (0.2 mM, 1.3 wt% in water). As a result, BSA nanoparticles of 200 nm average size with a size distribution between 100 and 300 nm was obtained (Figure 4). In

Figure 4. (A) SEM image of BSA nanoparticles prepared by addition of 4 mg of BSA aqueous solution (285 μL) at pH 9.0 to the $BmimBF_4$ (3 g) based system. (B) Particle size distribution obtained from the SEM image (A). Final BSA concentration is 0.02 mM. Mol% of water and $BmimBF_4$ are 53% and 44%, respectively.

addition, DLS provided their average size as around 450 nm in solution with a PDI 0.175 (Figure S2 (B). The sizes obtained from DLS are larger compare to the results obtained from SEM image, just like the results of sample obtained with 12 mg of BSA.

Lomis *et al.* showed that decreasing the BSA concentration in chloroform/water solution yields smaller BSA nanoparticles in the emulsion-solvent evaporation method.[2] Decreasing the BSA concentration leads to a decrease in the BSA-BSA

interactions. This avoids the formation of larger particles or agglomeration of BSA clusters. Also, BSA concentration directly affects the microviscosity of the system. Increasing the microviscosity in the nanodroplets with higher BSA concentration may cause additional resistance against applied shear stress during high-speed homogenization. This may hinder smaller nanodroplet formation. On the other hand, further decreasing the BSA content to 0.5 mg (0.025 mM, 0.16 wt%) in water did not yield albumin nanoparticles (Figure S3). A film-like formation was detected. This could be originated from the insufficient numbers of BSA to interact with and support to each other.

Effect of water volume on the albumin nanoparticle formation

BmimBF$_4$ is a hydrophilic ionic liquid, and it is macroscopically miscible with water at any concentrations. However, their mixtures are not homogeneous on the microscopic scale especially for the intermediate water contents (50 mol%).[34] Above the critical aggregation concentration (CAC = 0.45 M) of BmimBF$_4$, unstable mesostructures composed of water-rich and IL-rich domains were obtained.[31–33] Therefore, increasing the water content in BmimBF$_4$ phase produces water aggregates/pools. In Figure 3, we showed that 285 μL of water (53% mol) was used to solve BSA and then mixed with 3 g of BmimBF$_4$ (4.5 M, 44% mol) to obtain BSA nanoparticles.

However, dissolving the same amount of BSA (12 mg) in less or more water phase gave different results. Figure 5 (A)
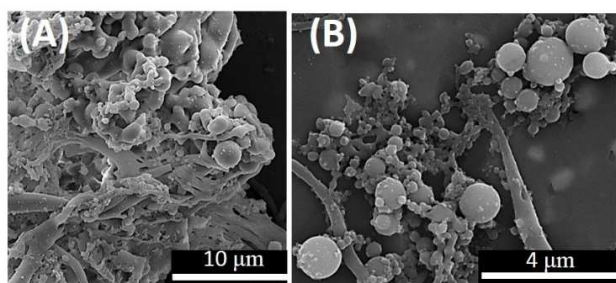
Figure 5. SEM images of BSA samples prepared by addition of 165 μL (A) and 525 μL (B) of BSA (12 mg) aqueous solutions to the BmimBF$_4$ based systems.

and (B) show the SEM images of BSA samples obtained upon addition of 165 μL (40% mol) and 525 μL (67% mol) of BSA containing water solutions into 3 g of BmimBF$_4$, respectively. In Figure 5 (A), mostly insoluble albumin aggregates were observed when 165 μL water (40% mol) was used. By decreasing the water content from 285 μL (53% mol) to 165 μL (40% mol), BSA concentration increases from 0.6 mM to 1.1 mM since 12 mg of BSA used for both conditions. It seems that during the albumin nanoparticle formation, close interactions between BSA proteins turned into larger aggregates with the help of glutaraldehyde cross linking process. On the other hand, by keeping the BSA amount constant, increasing the

volume of water phase from 285 μL (53% mol) to 525 μL (67% mol) produced larger BSA nanoparticles with non-uniform size distributions (Figure 5 (B)). This can be explained by the formation of larger water aggregates with increasing the water content. Also, applying the homogenizer with the same speed and time to a higher volume of water contained system might not be energetically successful to lead small nanoparticles with uniform size distributions.

**Effects of using glutaraldehyde and surfactants on the albumin nanoparticle formation**

As a cross-linker glutaraldehyde has been used mostly to stabilize the formed albumin nanoparticles.[8] It can cross-link proteins through amino acids with free amine sites such as lysine. Here, glutaraldehyde is required to stabilize the prepared albumin nanoparticles too. Without glutaraldehyde, albumin proteins form aggregates upon mixing with BmimBF$_4$ in the emulsion-like system (Figure S4). This shows the importance of using glutaraldehyde as cross-linker in this system to obtain stable albumin nanoparticles.

Furthermore, effects of surfactant (TX-100) and co-surfactant (1-butanol) on the albumin nanoparticle synthesis were studied. Surfactant molecules can decrease the interfacial tension between immiscible liquids in a system. This increases miscibility, colloidal stability and dispersion of nanoparticles in liquid.[34] In our system, BSA nanoparticle formation was not achieved without TX-100 and 1-butanol. As already shown in Figure 3 and 4, using 50 mM of non-ionic surfactant TX-100 (with 140 mM of 1-butanol) below its critical micelle concentration (CMC)[37] in BmimBF$_4$ helped to obtain BSA nanoparticles. Besides, using higher amount of surfactants such as 125 mM of TX-100 (with 420 mM of 1-butanol) caused BSA aggregation (Figure S5 (A)). Behera *et al.* showed that the CMC value of TX-100 increases with BmimBF$_4$ concentration in the aqueous solution.[37] At 30 wt% of BmimBF$_4$ solution, TX-100 does not form aggregation up to 50 mM of TX-100.[37] Therefore, in here, it is not expected to observe TX-100 (50 mM) aggregation in the 85 wt% of BmimBF$_4$ aqueous solution. But, 125 mM of TX-100 may form aggregation in our system and may cause the coalescence of BSA nanoparticles. This shows that the ratio of surfactants in the system plays a significant role for the BSA nanoparticle formation. In addition, Figure S5 (B) shows the role of the co-surfactant 1-butanol in this system. 1-butanol molecules may have aligned on the interface of the water/IL along with the TX-100 molecules and thus they enhanced water solubility of the obtained nanoparticles. Therefore, BSA aggregation was observed without using 1-butanol in the system (Figure S5 (B)).

Effects of alkyl chain lengths of ILs on the albumin nanoparticle formation

Structures of ILs-water mixtures are strongly dependent on the choice of the anion and cation. BF$_4^-$ ion containing imidazolium based ILs show hydrophilic properties, and their hydrophilicity decreases with increasing the alkyl chain lengths of

the imidazolium ring.[38] Therefore, in IL-water mixture, water pool formation increases with longer alkyl chain of IL. In addition, imidazolium types of ILs have denaturation effect on the albumin structure. Increasing the alkyl side chain of imidazolium cations leads to a higher albumin unfolding due to the enhanced hydrophobic interactions.[23] Here, we studied three imidazolium based ionic liquids (EmimBF$_4$, BmimBF$_4$ and HmimBF$_4$) with different alkyl chain lengths to obtain albumin nanoparticles. Addition of 4 mg BSA solution (285 μL water) into 3 g of EmimBF$_4$ in the presences of glutaraldehyde and surfactants did not produce BSA nanoparticles after applying the high-speed homogenizer. Figure 6 (A) shows the SEM
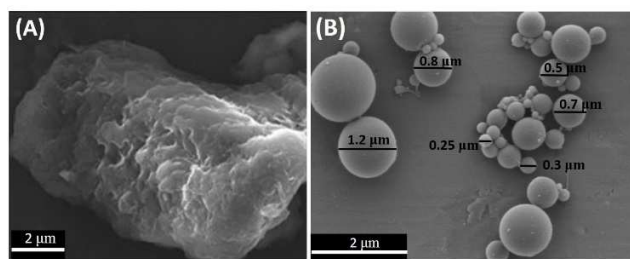
Figure 6. (A) SEM image of BSA aggregates obtained by using EmimBF$_4$ and (B) SEM image of BSA nanoparticles obtained by using HmimBF$_4$. 4 mg of BSA aqueous solution (285 μL) at pH 9.0 was added to the ILs (3 g) based system. Final BSA concentration is 0.015 mM. Mol% of water and ILs are 53% and 44%, respectively.

image of BSA aggregates obtained by using EmimBF$_4$. As already shown in Figure 3 and 4, BSA nanoparticles can be obtained in the BmimBF$_4$ based system. Increasing the alkyl side chain of imidazolium cation favors the polar/nonpolar nanophase separation in ILs. Therefore, water molecules can be aggregated in the polar regions of BmimBF$_4$ which stimulate the nanoparticle formation. Since the hydrophobicity of ethyl groups is not strong enough to create robust nonpolar domains in IL, water molecules can be homogeneously distributed in EmimBF4 more than in BmimBF4. Thus, they do not form water pools extensively in EmimBF$_4$ which are necessary for the albumin nanoparticle formation.

Further increasing the length of alkyl side chain of imidazolium cation from butyl to hexyl, water solubility decreases. Thus, this leads to larger water pools formation around the polar regions of HmimBF$_4$. Addition of 4 mg BSA solution (285 μL water) into 3 g of HmimBF$_4$ in the presences of glutaraldehyde and surfactants produce BSA nanoparticles after applying the high-speed homogenizer (Figure 6 (B)). As expected, larger water pools formed in the water-HmimBF$_4$ system leaded to the larger BSA nanoparticles compared to those formed in the water-BmimBF4 system. Spherical BSA nanoparticles with a broad size distribution between 0.2 μm and 1.2 μm were obtained in the water-HmimBF$_4$ micro-emulsion like system.

Conclusions

Organic solvents have been commonly used to prepare albumin nanoparticles. However, ionic liquids have been considered as green replacements for organic solvents due to their unique properties in addition to their designability features. Therefore, alternatively, here an imidazolium based ionic liquid of BmimBF$_4$ was used to prepare albumin nanoparticles.

It has been known that water in BmimBF$_4$ at intermediate levels (e.g. 50 mol%) forms water aggregates/pools.[31–34] These water aggregates are strongly dependent on the alkyl chain length of the imidazolium cation. Increasing the alkyl chain length forms larger water pools in the water-IL binary mixtures. Here, addition of BSA aqueous solution with glutaraldehyde into BmimBF$_4$ (with TX-100 and 1-butanol) forms an emulsion-like system upon applying high-speed homogenizer. Interactions between BmimBF$_4$ and BSA at the water/BmimBF$_4$ interface denature the BSA. After that, high-speed homogenization converted denatured BSA into BSA nanoparticles with the help of glutaraldehyde (Figure 2). By choosing the right experimental parameters including the pH value, concentration of BSA, volume of water solution and surfactant/co-surfactant ratios, smaller BSA nanoparticles (200 nm) with uniform size distribution can be obtained. Furthermore, using an IL with a shorter alkyl chain such as EmimBF$_4$ did not yield BSA nanoparticles, but using an IL with a longer alkyl chain, HmimBF$_4$, produced larger BSA nanoparticles with a broad size distribution. In more hydrophobic C$_n$mimBF$_4$ ionic liquids with n = 4 and 6, water pools were created upon addition of water at an intermediate level, which help nanoparticle formation. This shows the importance of water pools formation in the water-IL system for the BSA nanoparticle preparation. Here, we showed that ionic liquids can be good candidates for use in the preparation of albumin nanoparticles. The developed method is, of course, not restricted to bare albumin nanoparticle formation, could be applied to the field of drug loaded nanoparticles in the further studies.

Supporting Information Summary

Experimental details are given in the supporting information. Table S1 summarized the sample preparation. SEM images and DLS results were given in Figure S1 - S5.

Conflict of Interest

The authors declare no conflict of interest.

[1] A. O. Elzoghby, W. M. Samy, N. A. Elgindy, *J. Control. Release* **2012**, *157*, 168–182.

[2] N. Lomis, S. Westfall, L. Farahdel, M. Malhotra, D. Shum-Tim, S. Prakash, *Nanomaterials* **2016**, *6*, (116), 1–17.

[3] X. Tang, G. Wang, R. Shi, K. Jiang, L. Meng, H. Ren, J. Wu, Y. Hu, *Drug Deliv.* **2016**, *23*, 2686–2696.

[4] L. Zhang, S. Hou, S. Mao, D. Wei, X. Song, Y. Lu, *Int. J. Pharm.* **2014**, *287*, 155–162.

[5] J. S. Choi, N. Meghani, *Colloids Surf. B Biointerfaces* **2016**, *145*, 653–661.

[6] N. Desai, V. Trieu, Z. Yao, L. Louie, S. Ci, A. Yang, C. Tao, T. De, B. Beals, D. Dykes, P. Noker, R. Yao, E. Labao, M. Hawkins, P. Soon-Shiong, *Clin.Cancer Res.* **2006**, *12*, 1317–1324.

[7] K. Komiya, T. Nakamura, C. Nakashima, K. Takahashi, H. Umeguchi, N. Watanabe, A. Sato, Y. Takeda, S. Kimura, N. Sueoka-Aragane, *Onco. Targets Ther.* **2016**, *9*, 6663–6668.

[8] K. Langer, S. Balthasar, V. Vogel, N. Dinauer, H. Von Briesen, D. Schubert, *Int. J. Pharm.* **2003**, *257*, 169–180.

[9] B. Von Storp, A. Engel, A. Boeker, M. Ploeger, K. Langer, *J. Microencapsul.* **2012**, *29*, 138–146.

[10] L. Yang, F. Cui, D. Cun, A. Tao, K. Shi, W. Lin, W. , Int. *J. Pharm.* **2007**, *340*, 163–172.

[11] F. Crisante, I. Francolini, M. Bellusci, A. Martinelli, L. D'Ilario, A. Piozzi, *Eur. J. Pharm. Sci.* **2009**, *36*, 555–564.

[12] Q. Zhang, L. Zhang, L. Zemin, X. Xie, X. Gao, X. Xu, *AAPS Pharm. Sci. Tech.* **2017**, *18*, 2977–2986.

[13] N. Desai, Nanoparticle Albumin-Bound Paclitaxel (Abraxane®). In: M. Otagiri, V. Chuang (eds) Albumin in Medicine. **2016**, Springer, Singapore.

[14] Z. Qiu, J. Texter, *Curr. Opin. Colloid Interface Sci.* **2008**, *13*, 252–262.

[15] K. Ghandi, *Green Sustain. Chem.* **2014**, *4*, 44–53.

[16] S. Goindi, R. Kaur, R. Kaur, *Int. J. Pharm.* **2015**, *495*, 913–923.

[17] N. Adawiyah, M. Moniruzzaman, S. Hawatulaila, M. Goto, *Med. Chem. Comm.* **2016**, *7*, 1881–1897.

[18] J. Ghuman, P. A. Zunszain, I. Petitpas, A. A. Bhattacharya, M. Otagiri, S. Curry, *J. Mol. Biol.* **2005**, *353*, 38–52.

[19] F. Yang, C. Bian, L. Zhu, G. Zhao, Z. Huang, M. Huang, *J. Struct. Biol.* **2007**, *157*, 348–355.

[20] D. Tatlidil, M. Ucuncu, Y. Akdogan, *Phys. Chem. Chem. Phys.* **2015**, *17*, 22678–22685.

[21] Y. Akdogan, M. Emrullahoglu, D. Tatlidil, M. Ucuncu, G. Cakan-Akdogan, *Phys. Chem. Chem. Phys.* **2016**, *18*, 22531–22539.

[22] K. A. Majorek, P. J. Porebski, A. Dayal, M. D. Zimmerman, K. Jablonska, A. J. Stewart, M. Chruszcz, W. Minor, *Mol. Immunol.* **2012**, 52, 174–182.

[23] Y. Akdogan, M. J. N. Junk, D. Hinderberger, *Biomacromolecules* **2011**, *12*, 1072–1079.

[24] Y. Akdogan, D. Hinderberger, *J. Phys. Chem. B* **2011**, *115*, 15422–15429.

[25] J. Kuchlyan, N. Kundu, N. Sarkar, *Curr. Opin. Colloid Interface Sci.* **2016**, *25*, 27–38.

[26] G. Zhou, Z. Luo, X. Fu, *J. Agric. Food Chem.* **2014**, *62*, 8214–8220.

[27] G. Zhou, Z. Luo, X. Fu, *Ind. Crops Prod.* **2014**, *52*, 105–110.

[28] X. Wang, H. Chen, Z. Luo, X. Fu, *Carbohydr. Polym* **2016**, *138*, 192–200.

[29] T. Mendez-Morales, J. Carrete, O. Cabeza, L. J. Gallego, L. M. Varela, *J. Phys. Chem. B* **2011**, *115*, 6995–7008.

[30] Y. Akdogan, J. Heller, H. Zimmermann, D. Hinderberger, *Phys. Chem. Chem. Phys.* **2010**, *12*, 7874–7882.

[31] B. Wu, L. Zhang, Y. M. Zhang, H. P. Wang, *Chem. Eur. J.* **2009**, doi:10.1002/chem.200901098.

[32] D. R. Kattnig, Y. Akdogan, I. Lieberwirth, D. Hinderberger, *Mol. Phys.* **2013**, *111*, 2723–2737.

[33] D. R. Kattnig, Y. Akdogan, C. Bauer, D. Hinderberger, *Z. Phys. Chem.* **2012**, *226*, 1363–1378.

[34] K. Saihara, Y. Yoshimura, S. Ohta, A. Shimizu, *Sci. Reports* **2015**, *5*, 10619.

[35] S. Sebak, M. Mirzaei, M. Malhotra, A. Kulamarva, S. Prakash, *Int. J. Nanomed.* **2010**, *5*, 525–532.

[36] L. R. S. Barbosa, M. G. Ortore, F. Spinozzi, P. Mariani, S. Bernstorff, R. Itri, *Biophys. J.* **2010**, *98*, 147–157.

[37] K. Behera, M. D. Pandey, M. Porel, S. Pandey, *J. Chem. Phys.* **2007**, *127*, 184501.

[38] H. Heinz, C. Pramanik, O. Heinz, Y. Ding, R. K. Mishra, D. Marchon, R. J. Flatt, I. Estrela-Lopis, J. Llop, S. Moya, R. F. Ziolo, *Surf. Sci. Rep.* **2017**, *72*, 1–58.

[39] S. Feng, G. A. Voth, *Fluid Phase Equilib.* **2010**, *294*, 148–156.